THE VIRTUAL RESISTOR USED IN DROOP CONTROL OF DC MICROGRIDS IS A SERIES LOSS-FREE RESISTOR (SLFR)

Amanda L. Guerra, Ivo Barbi
Federal University of Santa Catarina, Florianópolis – SC, Brazil
e-mail: amandislg@gmail.com, ivobarbi@gmail.com

Abstract **– The recently introduced series loss-free resistor (SLFR) is used to obtain the non-linear differential equations that describe the dynamic response of a DC-DC converter with virtual resistor and input LC filter, employed in the voltage droop control of DC microgrids. The equilibrium point and the stability criteria of the converter are presented. The results of the theoretical analysis are validated via computer simulation of large-amplitude transients for step change of the input voltage, the output current and the voltage reference signal. It is shown that the energy absorbed by the virtual resistor is not converted into heat but returned to the input stage by a power source. Thus, the paradox of the virtual resistor, which causes a voltage drop but does not consume power, is resolved. This is a theoretical study.**

Keywords **– Dc Microgrids, Droop Control, Loss-free Resistor (LFR), Series Loss-free Resistor (SLFR), Virtual Resistor.**

I. INTRODUCTION

Droop control is a technique recognized for its importance in the decentralized control of direct current microgrids. It allows the coordination of the different components of the microgrid with high reliability since the regulation of the voltage of the distribution bus in direct current is not dependent on a single converter [1]-[3].

With the appropriate combination of parameters, droop control allows the power to be shared between different energy sources, proportional to their individual power capabilities, thus reducing the risk of failures [4].

Droop control also allows the various converters that make up the microgrid to operate in cooperation to regulate the voltage of the common direct current (DC) bus [5]-[7].

Another important assignment of droop control is the implementation of an active damping technique to overcome the negative instability resistance problem caused by the constant power loads (CPLs) [8]-[11].

The basic voltage droop control technique is implemented by means of voltage and current control algorithms, so that the output voltage of a converter linearly decreases with an increase in its load current. In this way, a virtual resistor of the appropriate value is emulated in each converter, which in the equivalent circuit is represented associated in series with the voltage source generated by the converter.

Manuscript received 08/03/2023; first revision 09/14/2023 and accepted for publication 09/14/2023, by recommendation of Editor Telles Brunelli Lazzarin. http://dx.doi.org/10.18618/REP.2023.3.0022

The concept of virtual resistor was introduced to provide damping of transient oscillations in the output of the *LC* filter of PWM inverters [12]. It was proposed by P. A. Dahono as a method to damp oscillations in the input LC filter of current-type AC-DC PWM converters [13] and to damp the oscillations of a DC-DC buck converter with an output *LCL* filter [14].

From an electric circuit perspective, the virtual resistor is a paradox, as it behaves like a conventional dissipative resistor when its effects are measured from the output terminals of the converter, causing voltage drop, and damping of the current and voltage oscillations, but without consuming power from the input power supply. This is a counterintuitive phenomenon. We can then deduce that the energy absorbed by the resistor, rather than being converted into heat by the Joule effect, is returned to the input stage of the circuit.

The concept of the loss-free resistor (LFR) was introduced by S. Singer [15], [16] and modeled by S. Singer and R. W. Erickson [17] using equivalent two-port networks for the buck, boost and buck-boost converters operating in discontinuous conduction mode (DCM), as shown in Figure 1.

The dipoles are formed by the effective resistor R_e and the power source P. The electrical power absorbed by the resistor is returned to the circuit by the power source. Therefore, the loss-free resistor affects the input and output characteristics of equivalent circuits, but without internal loss of energy.

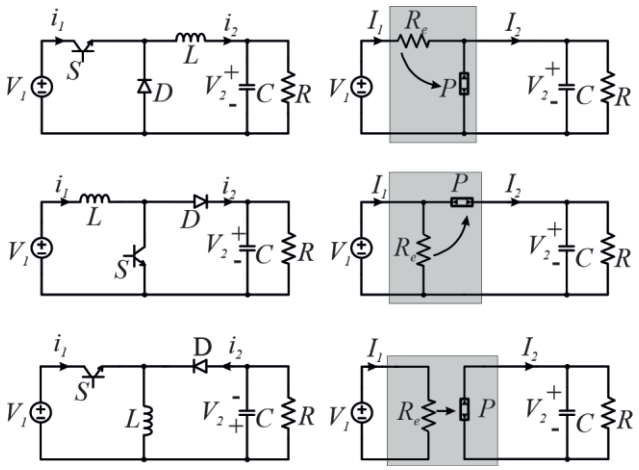

Fig. 1. The buck (a), boost (b) and buck-boost (c) dc-dc converters operating in discontinuous conduction mode and the respective averaged equivalent circuits using the power conservative loss-free resistor.

In the equivalent circuit of the buck converter shown in Figure 1.a, the resistor R_e is associated in series with the

input voltage source and the power source P is connected in parallel to the load. In the boost converter equivalent circuit, shown in Figure 1.b, the resistor R_e is connected in parallel to the input voltage and the power source P is associated in series with the output stage. In both cases the input and output ports are not decoupled. In the equivalent circuit of the buck-boost converter shown in Figure 1.c, the resistor R_e and the power source P are connected in parallel to the input source and the load respectively. Therefore, the input and output ports are decoupled from each other [17].

The resistor R_e is not associated in series with the load or the input power supply V_1 in any of the equivalent circuits shown in Figure 1. It can also be noted that in the three cases shown, the power source P is not connected in parallel to the source V_1. Therefore, in these cases the power consumed by resistor R_e is not returned to the input source V_1.

The recently introduced series loss-free resistor (SLFR) [18] consists of a loss-free resistor connected in series with the input voltage source and the load. The power source P is connected in parallel to the input voltage source V_1 and transfers to it all the power absorbed by the loss-free resistor R_e. The corresponding averaged equivalent circuit is shown in Figure 2.

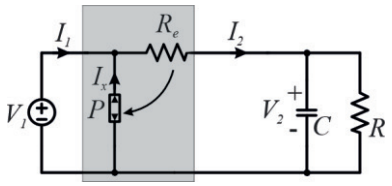

Fig. 2. Averaged equivalent circuit representation of the series loss-free resistor (SLFR).

A natural realization of the SLFR with no closed-loop control is possible with the use of the topological variation of the buck-boost converter with positive output voltage operating in DCM, as shown in Figure 3 [18].

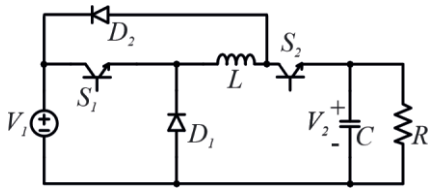

Fig. 3. Realization of the SLFR using a topological variation of the positive output voltage buck-boost converter operating in DCM.

In this article it is demonstrated that the virtual resistor used to perform the droop control in direct current microgrids is a series loss-free resistor (SLFR). Using this concept, nonlinear differential equations are obtained that correctly describe the behavior of the converter both in steady state and with large-amplitude transients. In addition, the determination of equilibrium points and stability criteria when an input filter is used is described.

II. MODELLING THE BUCK CONVERTER WITH VIRTUAL RESISTOR AND INPUT FILTER

A schematic diagram of the buck converter with a virtual resistor and input filter is shown in Figure 4.

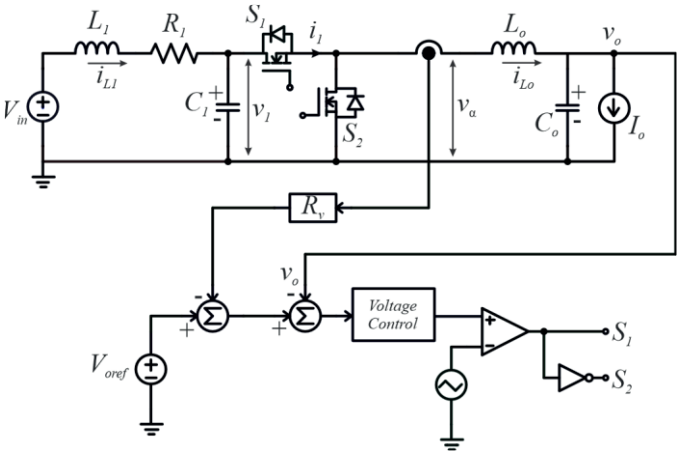

Fig. 4. Buck converter with virtual resistor R_v and input LC filter.

To simplify the analysis, let us assume that the output stage formed by R_v, L_o and C_o are overdamped, which implies that:

$$\frac{R_v}{2L_o} > \frac{1}{\sqrt{L_o C_o}} . \tag{1}$$

Furthermore, it will also be considered that the control of the output voltage is very fast in relation to the cutoff frequency of the input filter, formed by R_1, L_1 and C_1. This hypothesis allows a reduction in the system order and the simplification of the model.

We can then write, for quasi-instantaneous average values,

$$v_\alpha = V_{oref} - R_v\, i_{Lo} \tag{2}$$

where R_v is the realized virtual resistance of the buck converter, i_{Lo} is the current in the inductor L_o, v_α is the voltage before the inductor, and V_{oref} is the reference voltage.

Let the power p_α be defined by:

$$p_\alpha = v_\alpha\, i_{Lo} . \tag{3}$$

Substituting (2) in (3) we find:

$$p_\alpha = V_{oref}\, i_{Lo} - R_v\, i_{Lo}^2 . \tag{4}$$

The power p_1 is given by:

$$p_1 = v_1\, i_1 \tag{5}$$

As power semiconductors are considered ideal, $p_1 = p_\alpha$. Thus, equating (4) and (5) and rearranging the terms of the equation, we obtain:

$$i_1 = \frac{V_{oref}\, i_{Lo}}{v_1} - \frac{p_v}{v_1} \tag{6}$$

where p_v is the power consumed by the virtual resistor given by:

$$p_v = R_v\, i_{Lo}^2 . \tag{7}$$

Equations (2), (6) and (7) represent the equivalent circuit shown in Figure 5.

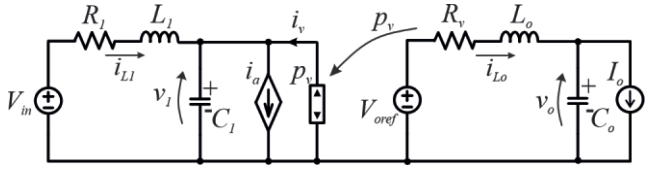

Fig. 5. Averaged equivalent circuit of the buck converter with virtual resistor R_v and input LC filter, in terms of the series loss-free resistor (SLFR).

The currents i_a and i_v are given by (8) and (9), respectively.

$$i_a = \frac{V_{oref}\, i_{Lo}}{v_1} \tag{8}$$

$$i_v = \frac{p_v}{v_1}. \tag{9}$$

As the equivalent circuit shows, the electrical energy absorbed by the virtual resistor R_v is not converted into heat but recycled to the input stage by the power source P_v. Therefore, as shown in [18], the virtual resistor is a series loss-free resistor (SLFR).

A. Mathematical Model

The equivalent circuit shown in Figure 4 is described by the system of nonlinear differential equations.

$$\frac{dv_o}{dt} = \frac{1}{C_o}\left(i_{Lo} - I_o\right) \tag{10}$$

$$\frac{di_{Lo}}{dt} = \frac{1}{L_o}\left(V_{oref} - R_v\, i_{Lo} - v_o\right) \tag{11}$$

$$\frac{dv_1}{dt} = \frac{1}{C_1}\left(i_{L1} + \frac{R_v\, i_{Lo}^2}{v_1} - \frac{V_{oref}\, i_{Lo}}{v_1}\right) \tag{12}$$

$$\frac{di_{L1}}{dt} = \frac{1}{L_1}\left(V_{in} - R_1\, i_{L1} - v_1\right). \tag{13}$$

The equilibrium point is found by making $\frac{dv_o}{dt} = \frac{di_{Lo}}{dt} = \frac{dv_1}{dt} = \frac{di_1}{dt} = 0$ in equations (10), (11), (12) and (13), which results in the system of algebraic equations.

$$0 = \frac{1}{C_o}\left(i_{L_o}^* - I_o\right) \tag{14}$$

$$0 = \frac{1}{L_o}\left(V_{oref} - R_v\, i_{Lo}^* - v_o^*\right) \tag{15}$$

$$0 = \frac{1}{C_1}\left(i_{L1}^* + \frac{R_v\, i_{Lo}^{*\,2}}{v_1^*} - \frac{V_{oref}\, i_{Lo}^*}{v_1^*}\right) \tag{16}$$

$$0 = \frac{1}{L_1}\left(V_{in} - R_1\, i_{L1}^* - v_1^*\right). \tag{17}$$

Solving the system of algebraic equations, we find two equilibrium points. However, herein we will only discuss the equilibrium point that is of practical interest, given by:

$$i_{L_o}^* = I_o \tag{18}$$

$$v_o^* = V_{oref} - R_v\, i_{Lo}^* \tag{19}$$

$$v_1^* = \frac{V_{in}}{2} + \sqrt{\left(\frac{V_{in}}{2}\right)^2 + R_1 R_v I_o^2 - R_1 V_{oref}\, I_o} \tag{20}$$

$$i_{L1}^* = \frac{1}{R_1}\left(\frac{V_{in}}{2} - \sqrt{\left(\frac{V_{in}}{2}\right)^2 + R_1 R_v I_o^2 - R_1 V_{oref}\, I_o}\right) \tag{21}$$

where i^*_{Lo}, i^*_{L1}, v^*_1 and v^*_o are the values of the currents in the inductors and the voltages in the capacitors at the equilibrium point.

The equivalent circuit for the converter operating at the equilibrium is shown in Figure 6, where i^*_a, p^*_v and i^*_v are given by (22), (23) and (24), respectively.

$$i_a^* = \frac{V_{oref}\, I_o}{v_1^*} \tag{22}$$

$$p_v^* = R_v I_o^2 \tag{23}$$

$$i_v^* = \frac{p_v^*}{v_1^*}. \tag{24}$$

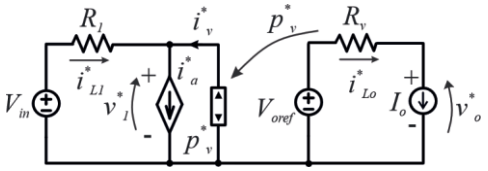

Fig. 6. Averaged equivalent circuit at the equilibrium point described by equations (18), (19), (20) and (21).

III. LARGE SIGNAL TRANSIENTS

To validate the mathematical model obtained using the SLFR concept, this section presents simulation results for the circuits shown in Figures 4 and 5, with parameters V_{oref} = 50 V, L_1 = 1 mH, R_1 = 0.25 Ω, C_1 = 1mF, R_v = 4 Ω, L_o = 250 µH,
C_o = 100 µF and f_s = 20 kHz. Voltage and current sensors with unity gains are used.

To control the voltage of the converter, a PI controller described by the transfer function is used, as follows.

$$G_v(s) = 0.01 + \frac{100}{s}. \quad (25)$$

A. Large Signal Transient for a Step Change of the Input Voltage.

In this section, the transient response of the converter to a large-amplitude variation in the input voltage V_{in} (in the form of a step) is analyzed, with the reference voltage kept constant. The load is represented by the current source I_o = 5 A. The input voltage before the step change is V_{in} = 100 V. At the instant t = 30 ms the value of the input voltage is increased to V_{in} = 120 V.

The equilibrium point for V_{in} = 100 V is given by i^*_{Lo} =*5A*, i^*_{L1} = *1.506A*, v^*_1 = *99.624V* and v^*_o = *30V*. At this operating point γ = 0.25 and β = -1.509. As γ > -β, the system is stable at this equilibrium point. The parameters γ and β are defined in Section IV of this manuscript.

The equilibrium point for V_{in} = 120 V is given by i^*_{Lo} =*5A*, i^*_{L1} = *1.253A*, v^*_1 = *119.687V* and v^*_o = *30V*. At this operating point γ = 0.25 and β = -1.255. Therefore γ > -β and the system is also stable at this equilibrium point.

The converter shown in Figure 4 and its large amplitude equivalent circuit represented in Figure 5 were simulated using PSIM software and the relevant waveforms are shown in Figure 7.

It can be observed that there are no differences between the waveforms for the two circuits, which validates the proposed model for transients caused by a large-amplitude disturbance in the step form of the input voltage V_{in}.

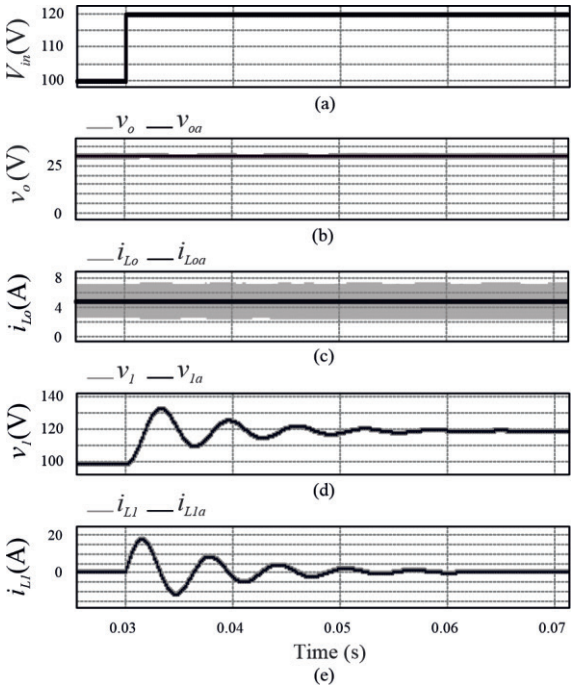

Fig. 7. Computer generated waveforms. (a) Input voltage V_{in}. (b) Output voltage for the switched converter (v_o) and the averaged equivalent circuit (v_{oa}). (c) Current through the inductor L_o for the switched converter (i_{Lo}) and the equivalent circuit (i_{Loa}). (d) Voltage across an input filter capacitor for the switched converter (v_1) and the averaged equivalent circuit (v_{1a}). (e) Current through the input inductor for the switched converter (i_{L1}) and the equivalent circuit (i_{L1a}).

B. Large Signal Transient for a Step Change of the Load Current

In this section simulation results are presented for the switched converter and its equivalent circuit, shown in Figures. 4 and 5 respectively. The input voltage V_{in} is constant and the load current source I_o, initially equal to *3A*, is increased to *8A* at the instant t = 50 ms.

The equilibrium point for I_o = *3A* is given by i^*_{Lo} =*3A*, i^*_{L1} = *1.143A*, v^*_1 = *99.71V* and v^*_o = *38V*. For I_o = *8A*, the states at the equilibrium point are i^*_{Lo} =*8A*, i^*_{L1} = *1.445A*, v^*_1 = *99.64V* and v^*_o = *18V*. At both equilibrium points the system is stable.

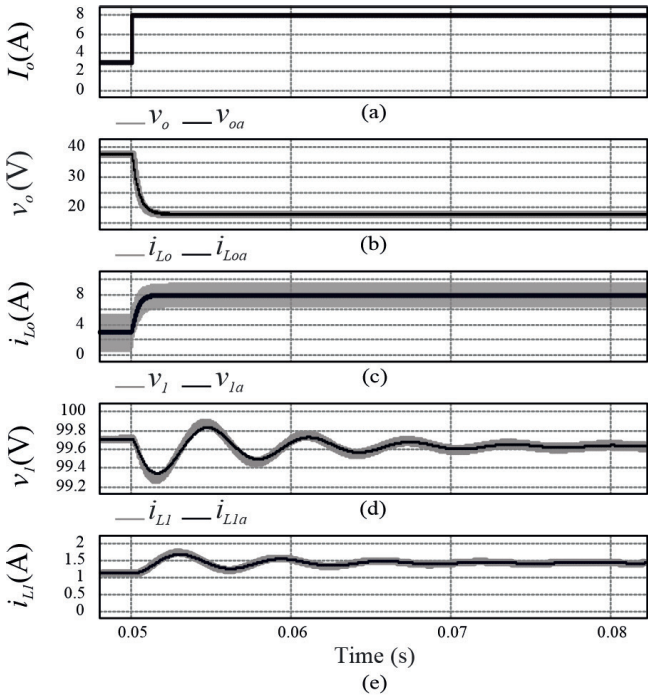

Fig. 8. Computer generated waveforms. (a) Load current I_o. (b) Output voltage for the switched converter (v_o) and the averaged equivalent circuit (v_{oa}). (c) Current through the inductor for the switched converter (i_{Lo}) and the equivalent circuit (i_{Loa}). (d) Voltage across an input filter capacitor for the switched converter (v_1) and the averaged equivalent circuit (v_{1a}). (e) Current through the input inductor for the switched converter (i_{L1}) and the equivalent circuit (i_{L1a}).

The relevant waveforms for this large-amplitude disturbance in the load current are shown in Figure 8. In this case, the proposed model, based on SLFR, once again correctly describes the converter behavior.

Figure 9 shows simulation results when p_v = 0. This means that the energy consumed by the virtual resistor R_v is not returned to the input source but converted into heat. Note that this condition does not modify the behavior of v_o and i_{Lo}.

However, there is a significant difference in the behavior of v_1 and i_{L1}, which shows that the proposed model is correct and that it also describes the behavior of the converter for large-amplitude transients for this type of disturbance.

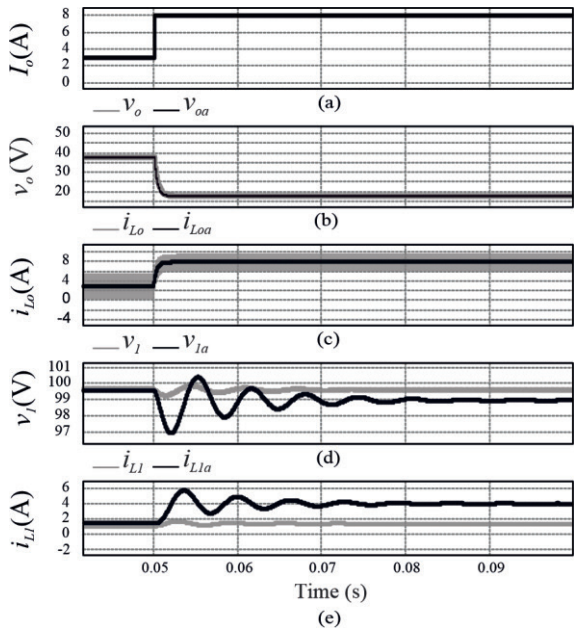

Fig. 9. Computer generated waveforms, without the power source P_v. (a) Load current I_o. (b) Output voltage for the switched converter (v_o) and the averaged equivalent circuit (v_{oa}). (c) Current through the inductor L_o for the switched converter (i_{Lo}) and the equivalent circuit (i_{Loa}). (d) Voltage across an input filter capacitor for the switched converter (v_1) and the averaged equivalent circuit (v_{1a}). (e) Current through the input inductor for the switched converter (i_{L1}) and the equivalent circuit (i_{L1a}).

C. Large Signal Transient for a Step Change of the Reference Voltage

Both circuits were simulated, and the waveforms generated by computer simulation are shown in Figure 10.

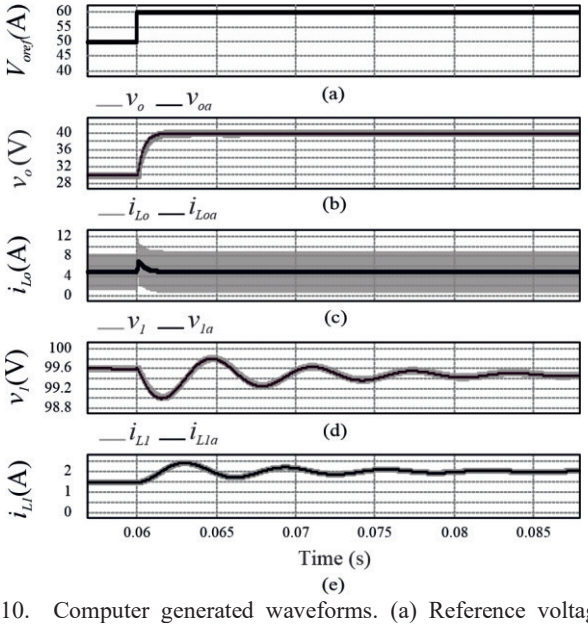

Fig. 10. Computer generated waveforms. (a) Reference voltage V_{oref}. (b) Output voltage for the switched converter (v_o) and the averaged equivalent circuit (v_{oa}). (c) Current through the inductor L_o for the switched converter (i_{Lo}) and the equivalent circuit (i_{Loa}). (d) Voltage across the input filter capacitor for the switched converter (v_1) and the averaged equivalent circuit (v_{1a}). (e) Current through the input inductor L_1 for the switched converter (i_{L1}) and the averaged equivalent circuit (i_{L1a}).

The simulation was done with the same parameters presented in the situations previously described, but with V_{in} = 100 V and I_o = 5 A. At instant t = 60 ms, when the circuit is at an equilibrium point, a step change in the magnitude of the reference voltage takes place, from V_{oref} = 50 V to V_{oref} = 60 V. It can be noted that the waveforms generated by computer simulation for the two circuits are identical.

Figure 11 shows the same waveforms as Figure 10, making P_v = 0. Hence, the energy consumed by resistor R_v is converted into heat and does not return to the input voltage source. Thus, this condition leads to erroneous results.

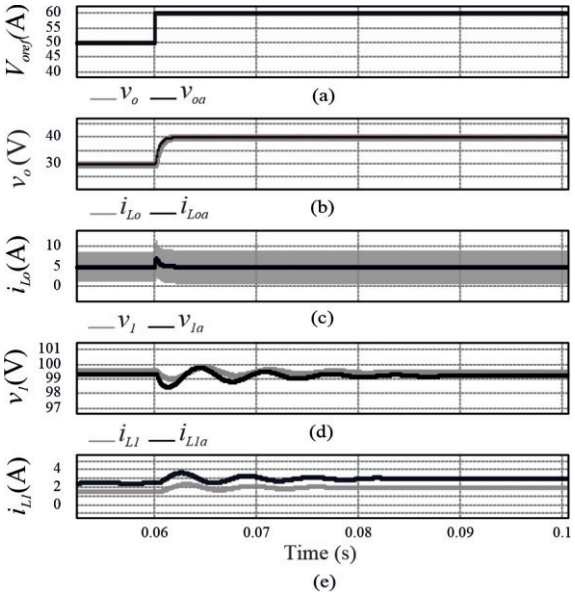

Fig. 11. Computer generated waveforms for a step change of the reference voltage with P_v = 0.

IV. STABILITY ANALYSIS

The equilibrium point, given by (18), (19), (20) and (21) was determined by performing the static analysis of the converter. Dynamic analysis is necessary to determine the combination of parameters that ensure equilibrium point stability. The local stability at an equilibrium point is studied by evaluating the Jacobian matrix, given by:

$$J = \begin{pmatrix} \frac{\partial F_1}{\partial v_o} & \frac{\partial F_2}{\partial v_o} & \frac{\partial F_3}{\partial v_o} & \frac{\partial F_4}{\partial v_o} \\ \frac{\partial F_1}{\partial i_{Lo}} & \frac{\partial F_2}{\partial i_{Lo}} & \frac{\partial F_3}{\partial i_{Lo}} & \frac{\partial F_4}{\partial i_{Lo}} \\ \frac{\partial F_1}{\partial v_1} & \frac{\partial F_2}{\partial v_1} & \frac{\partial F_3}{\partial v_1} & \frac{\partial F_4}{\partial v_1} \\ \frac{\partial F_1}{\partial i_{L1}} & \frac{\partial F_2}{\partial i_{L1}} & \frac{\partial F_3}{\partial i_{L1}} & \frac{\partial F_4}{\partial i_{L1}} \end{pmatrix} \quad (26)$$

where $F_1 = \frac{dv_o}{dt}$, $F_2 = \frac{di_{Lo}}{dt}$, $F_3 = \frac{dv_1}{dt}$ and $F_4 = \frac{di_{L1}}{dt}$.

Carrying out the indicated partial derivations and substituting in (26), for the equilibrium point we obtain:

$$J = \begin{pmatrix} 0 & -\frac{1}{L_o} & 0 & 0 \\ \frac{1}{C_o} & -\frac{R_v}{L_o} & -\frac{\alpha}{C_1} & 0 \\ 0 & 0 & -\frac{\beta}{C_1} & -\frac{1}{C_1} \\ 0 & 0 & \frac{1}{C_1} & -\frac{R_1}{L_1} \end{pmatrix} \quad (27)$$

where:

$$\alpha = \frac{V_{oref} - 2R_v I_o}{\frac{V_{in}}{2} + \sqrt{\left(\frac{V_{in}}{2}\right)^2 + R_1 R_v I_o - R_1 V_{oref} I_o}} \quad (28)$$

and

$$\beta = \frac{R_v I_o^{\,2} - V_{oref} I_o}{\left[\frac{V_{in}}{2} + \sqrt{\left(\frac{V_{in}}{2}\right)^2 + R_1 R_v I_o - R_1 V_{oref} I_o}\right]^2} . \quad (29)$$

The eigenvalues of the Jacobian matrix for the converter at the equilibrium point are:

$$\lambda_{1,2} = -\left(\frac{R_1}{2L_1} + \frac{\beta}{2C1}\right) \pm j\sqrt{\left(\frac{R_1}{2L_1}\right)^2 - \frac{R_1\beta}{2C_1L_1} - \frac{1}{C_1L_1} + \left(\frac{\beta}{2C1}\right)^2}$$

(30)

$$\lambda_{3,4} = -\frac{R_v}{2L_o} \pm j\sqrt{\left(\frac{R_v}{2L_o}\right)^2 - \frac{1}{C_oL_o}} . \quad (31)$$

As $R_v > 0$ and $L_o > 0$, the real part of the eigenvalues $\lambda_{3,4}$ is always negative, that is, $\mathrm{Re}(\lambda_{3,4}) < 0$.

The real part of the eigenvalues $\lambda_{1,2}$ is given by:

$$\mathrm{Re}\left(\lambda_{1,2}\right) = -\left(\frac{R_1}{2L_1} + \frac{\beta}{2C_1}\right) . \quad (32)$$

For the system to be asymptotically stable, it must be true that $\mathrm{Re}(\lambda_{1,2}) < 0$, which implies that:

$$\left(\frac{R_1}{2L_1} + \frac{\beta}{2C_1}\right) > 0 . \quad (33)$$

We can then conclude that this condition occurs when:

$$\gamma > -\beta \quad (34)$$

where:

$$\gamma = \frac{R_1 C_1}{L_1} . \quad (35)$$

A. Case Study

Let us consider a converter with the parameters V_{oref} = 50 V, L_1 = 20 mH, R_1 = 0.25 Ω, C_1 = 1 mF, R_v = 4 Ω, L_o = 150 µH, and C_o = 100 µF. Substituting these values in (35) we find γ = 0.013. In Figure 12 γ and $-\beta(I_o)$ are plotted. The curves indicate that for the given parameters, the system is unstable for $3.45A \le I_o \le 9.02A$, the region where $\gamma < -\beta$.

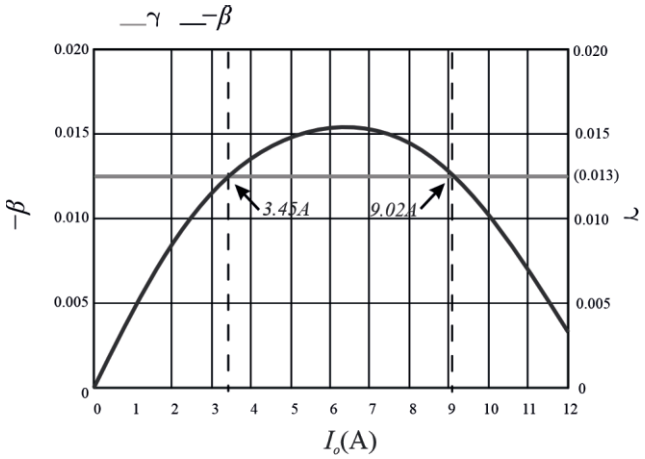

Fig. 12. Graph of γ and $-\beta(Io)$.

Simulation results are shown in Figure 13, for the converter and its equivalent circuit in terms of SLFR.

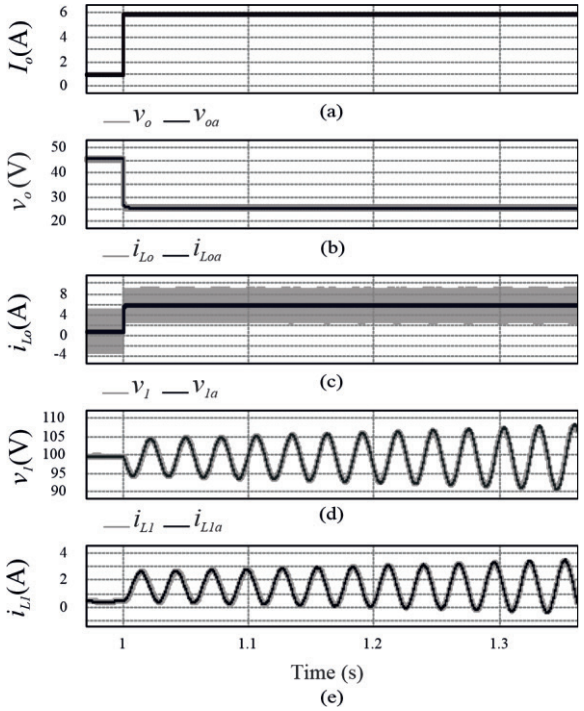

Fig. 13. Unstable behavior in response to a step change of the current I_o from *1A* to *6A*.

When t < 1 s, the load current is I_o = *1A* and β = -0.00465.

Since $\gamma > -\beta$, the system is stable. At the instant $t = 1$ s the value of the current is increased to $I_o = 6A$, which substituted in (29) yields $\beta = -0.0157$. As $\gamma < -\beta$, the system becomes unstable.

The effect of instability is observed in the behavior of the voltage v_1 and current i_{L1} that theoretically increase indefinitely. We can see that the results obtained for the original switching converter and its equivalent circuit in terms of SLFR are identical.

V. CONCLUSION

In this paper it is demonstrated that the virtual resistor used in the droop control of DC microgrids is a series loss-free resistor (SLFR).

The behavior of the converter with an input LRC filter is described by a system of nonlinear differential equations that has no analytical solution. Through the analysis, a criterion is presented for the verification of local stability in the vicinity of the equilibrium point.

The analysis reveals, as confirmed by computer simulation, that the converter can become unstable and that this is not only dependent of the parameters of the circuit but also on the nature of the load.

The analysis results are validated by computer simulation for large-amplitude transients in response to a step change in the input voltage, the output current and the reference signal of the load voltage control.

The proposed modeling method using the SLFR can also be applied to other isolated or non-isolated DC-DC converters, used to perform droop control in direct current microgrids.

The mathematical model obtained and the corresponding averaged equivalent circuit in terms of the SLFR, are appropriate tools for analyzing and sizing a converter that performs virtual resistance in various applications, particularly in DC microgrids and renewable energy power systems.

It therefore appears that the proposed method for describing the behavior of the DC-DC converters with virtual resistor resolves the virtual resistor paradox.

REFERENCES

[1] I. Batarseh, K. Siri and H. Lee, "Investigation of the output droop characteristics of parallel-connnected DC-DC converters", in *Proceedings of 1994 Power Electronics Specialist Conference - PESC'94*, vol.2, pp. 1342-1351, July 1994, doi: 10.1109/PESC.1994.373859.

[2] Z. Moussaoui, I. Batarseh, H. Lee and C. Kennedy, "An overview of the control scheme for distributed power systems", in *Southcon/96 Conference Record*, pp. 584-591, July 1996, doi: 10.1109/SOUTHC.1996.535130.

[3] S. Anand, B. G. Fernandes and J. Guerrero, "Distributed Control to Ensure Proportional Load Sharing and Improve Voltage Regulation in Low-Voltage DC Microgrids", *IEEE Transactions on Power Electronics*, vol. 28, no. 4, pp. 1900-1913, Apr. 2013, doi: 10.1109/TPEL.2012.2215055.

[4] T. Dragičević, X. Lu, J. C. Vasquez and J. M. Guerrero, "DC Microgrids—Part I: A Review of Control Strategies and Stabilization Techniques", *IEEE Transactions on Power Electronics*, vol. 31, no. 7, pp. 4876-4891, July 2016, doi: 10.1109/TPEL.2015.2478859.

[5] S. Peyghami, H. Mokhtari and F. Blaabjerg, "Decentralized Load Sharing in a Low-Voltage Direct Current Microgrid with an Adaptive Droop Approach Based on a Superimposed Frequency", *IEEE Journal of Emerging and Selected Topics in Power Electronics*, vol. 5, no. 3, pp. 1205-1215, Sept. 2017, doi: 10.1109/JESTPE.2017.2674300.

[6] E. Espina, J. Llanos, C. Burgos-Mellado, R. Cárdenas-Dobson, M. Martínez-Gómez and D. Sáez, "Distributed Control Strategies for Microgrids: An Overview", *IEEE Access*, vol. 8, pp. 193412-193448, Oct.-Nov. 2020, doi: 10.1109/ACCESS.2020.3032378.

[7] W. Xie, M. Han, W. Cao, J. M. Guerrero and J. C. Vasquez, "Virtual Resistance Tradeoff Design for DCMG Grid-Forming Converters Considering Static- and Large-Signal Dynamic Constraints", *IEEE Transactions on Power Electronics*, vol. 36, no. 5, pp. 5582-5593, May 2021, doi: 10.1109/TPEL.2020.3029716.

[8] A. M. Rahimi and A. Emadi, "Active Damping in DC/DC Power Electronic Converters: A Novel Method to Overcome the Problems of Constant Power Loads", *IEEE Transactions on Industrial Electronics*, vol. 56, no. 5, pp. 1428-1439, May 2009, doi: 10.1109/TIE.2009.2013748.

[9] A. Kwasinski and C. N. Onwuchekwa, "Dynamic Behavior and Stabilization of DC Microgrids With Instantaneous Constant-Power Loads", *IEEE Transactions on Power Electronics*, vol. 26, no. 3, pp. 822-834, Mar. 2011, doi: 10.1109/TPEL.2010.2091285.

[10] Mingfei Wu and D. D. C. Lu, "Adding virtual resistance in source side converters for stabilization of cascaded connected two stage converter systems with constant power loads in DC microgrids", in *International Power Electronics Conference (IPEC-Hiroshima 2014 - ECCE ASIA)*, pp. 3553-3556, 2014 doi: 10.1109/IPEC.2014.6870007.

[11] A. P. N. Tahim, D. J. Pagano, E. Lenz and V. Stramosk, "Modeling and Stability Analysis of Islanded DC Microgrids Under Droop Control", *IEEE Transactions on Power Electronics*, vol. 30, no. 8, pp. 4597-4607, Aug. 2015, doi: 10.1109/TPEL.2014.2360171.

[12] P. A. Dahono, Y. R. Bahar, Y. Sato and T. Kataoka, "Damping of transient oscillations on the output LC filter of PWM inverters by using a virtual resistor", in *4th IEEE International Conference on Power Electronics and Drive Systems. IEEE PEDS 2001 - Indonesia. Proceedings (Cat. No.01TH8594)*, vol.1, pp. 403-407, 2001, doi: 10.1109/PEDS.2001.975347.

[13] P. A. Dahono, "A method to damp oscillations on the input LC filter of current-type AC-DC PWM converters by using a virtual resistor", in *The 25th International Telecommunications Energy Conference, 2003. INTELEC '03.*, pp. 757-761, 2003.

[14] P. A. Dahono, "A control method for DC-DC converter that has an LCL output filter based on new virtual capacitor and resistor concepts", in *35th Annual Power Electronics Specialists Conference (IEEE Cat.*

No.04CH37551), vol.1, pp. 36-42, June 2004, doi: 10.1109/PESC.2004.1355709.

[15] S. Singer, "Realization of loss-free resistive elements", *IEEE Transactions on Circuits and Systems*, vol. 37, no. 1, pp. 54-60, Jan. 1990, doi: 10.1109/31.45691.

[16] S. Singer, "The application of 'loss-free resistors' in power processing circuits", in *20th Annual IEEE Power Electronics Specialists Conference, Milwaukee, WI, USA*, vol.2, pp. 843-846, June 1989, doi: 10.1109/PESC.1989.48568.

[17] S. Singer and R. W. Erickson, "Canonical modeling of power processing circuits based on the POPI concept", *IEEE Transactions on Power Electronics*, vol. 7, no. 1, pp. 37-43, Jan. 1992, doi: 10.1109/63.124575.

[18] I. Barbi, "Series Loss-Free Resistor: Analysis, Realization, and Applications", *IEEE Transactions on Power Electronics*, vol. 36, no. 11, pp. 12857-12866, Nov. 2021, doi: 10.1109/TPEL.2021.3082509.

BIOGRAPHIES

Amanda Lahera was born in Marianao, Havana, Cuba. She received the B.S degree in Automation and Control systems engineering from the Technological University of Havana, Cuba, in 2018. She received the M.S degree in electrical engineering from the Federal University of Santa Catarina (UFSC), Florianópolis, Brazil, in 2021. She is currently a doctoral student at the Federal University of Santa Catarina, Brazil.

Ivo Barbi (*Life Fellow*, IEEE) was born in Gaspar, Brazil. He received the B.S. and M.S. degrees in electrical engineering from the Federal University of Santa Catarina (UFSC), Florianópolis, Brazil, in 1973 and 1976, respectively, and the Dr. Ing. degree in electrical engineering from the Institute National Polytechnique de Toulouse (INPT), Toulouse, France, in 1979. He founded the Brazilian Power Electronics Society (SOBRAEP), the Brazilian Power Electronics Conference (COBEP), in 1990, and the Brazilian Power Electronics and Renewable Energy Institute (IBEPE), in 2016. He is currently a Researcher with the Solar Energy Research Center and a Professor Emeritus in electrical engineering with UFSC. Prof. Barbi received the 2020 IEEE William E. Newell Power Electronics Award. He served as an Associate Editor for the IEEE TRANSACTIONS ON INDUSTRIAL ELECTRONICS and the IEEE TRANSACTIONS ON POWER ELECTRONICS for several years. He is currently Editor for the electrical engineering area of the SCIENTIFIC REPORTS JOURNAL (Springer-Nature) and Associate Editor of the JOURNAL OF CONTROL, AUTOMATION AND ELECTRICAL SYSTEMS.